



HAL
open science

Simulations of Dense Granular Flow: Dynamic Arches and Spin Organization

S. Luding, J. Duran, E. Clément, J. Rajchenbach

► **To cite this version:**

S. Luding, J. Duran, E. Clément, J. Rajchenbach. Simulations of Dense Granular Flow: Dynamic Arches and Spin Organization. *Journal de Physique I*, 1996, 6 (6), pp.823-836. 10.1051/jp1:1996244 . jpa-00247217

HAL Id: jpa-00247217

<https://hal.science/jpa-00247217>

Submitted on 4 Feb 2008

HAL is a multi-disciplinary open access archive for the deposit and dissemination of scientific research documents, whether they are published or not. The documents may come from teaching and research institutions in France or abroad, or from public or private research centers.

L'archive ouverte pluridisciplinaire **HAL**, est destinée au dépôt et à la diffusion de documents scientifiques de niveau recherche, publiés ou non, émanant des établissements d'enseignement et de recherche français ou étrangers, des laboratoires publics ou privés.

Simulations of Dense Granular Flow: Dynamic Arches and Spin Organization

S. Luding ^(1,*), J. Duran ⁽²⁾, E. Clément ⁽²⁾, J. Rajchenbach ⁽²⁾

⁽¹⁾ Institut für Computeranwendungen 1, Pfaffenwaldring 27, 70569 Stuttgart, Germany

⁽²⁾ Laboratoire d'Acoustique et d'Optique de la Matière Condensée (**),
Université Pierre et Marie Curie, 4 place Jussieu, 75252 Paris Cedex 05, France

(Received 1st December 1995, revised 1st February 1996, accepted 26 February 1996)

PACS.46.10.+z – Mechanics of discrete systems

PACS.05.60+w – Transport processes: theory

PACS.47.20-k – Hydrodynamic stability

Abstract. — We present a numerical model for a two dimensional (2D) granular assembly, falling in a rectangular container when the bottom is removed. We observe the occurrence of cracks splitting the initial pile into pieces, like in experiments. We study in detail various mechanisms connected to the “discontinuous decompaction” of this granular material. In particular, we focus on the history of one single long range crack, from its origin at one side wall, until it breaks the assembly into two pieces. This event is correlated to an increase in the number of collisions, i.e. strong pressure, and to a momentum wave originated by one particle. Eventually, strong friction reduces the falling velocity such that the crack may open below the slow, high pressure “dynamic arch”. Furthermore, we report the presence of large, organized structures of the particles’ angular velocities in the dense parts of the granulate when the number of collisions is large.

1. Introduction

The flow behavior of granular media in hoppers, pipes or chutes has received increasing interest during the last years. For a review concerning the physics of granular materials, see [1,2] and references therein.

The complete dynamical description of gravity driven flows is an open problem and for geometries like hoppers or vertical pipes, several basic phenomena, are still unexplained. In hoppers intermittent clogging due to vault effects [3], density waves in the bulk [4] or $1/f$ noise of the outlet pressure, have been reported from experiments [5]. In a vertical pipe geometry, numerical simulations on model systems with periodic boundary conditions [6,7] and also analytical studies [8] show density waves. But so far, experimental evidence of density waves is only found in situations where pneumatic effects, *i.e.* gas-particle interactions, are important [9].

In the rapid flow regime, kinetic theories [10,11] describe the behavior of the system introducing the granular temperature as a measure of the velocity fluctuations. In quasistatic

(*) Author for correspondence (e-mail: lui@ica1.uni-stuttgart.de)

(**) URA 800 CNRS

situations, also arching effects and particle geometry get to be important. Under those conditions, kinetic theories and also continuum soil mechanics do not completely describe all the phenomena observed. The complicated particle-wall and particle-particle interactions [12–14], possible formation of stress chains in the granulate and also stress fluctuations [15,16] undoubtedly require further experimental, theoretical and simulation work.

Following recent research on model granular systems [15–21] we focus here on the problem of a 2D pile made up of rather large spheres enclosed in a rectangular container with transparent front and back walls, separated by slightly more than one particle diameter. Recent observations of approximately V-shaped *microcracks* in vertically vibrated sand-piles [17] were complemented by recent experiments and simulations of the discontinuous decompaction of a falling sandpile [22]. From experiments Duran *et al.* [22] find the following basic features: in a system with polished laterals walls, cracks are unlikely to appear during the fall, *i.e.* the pile will accelerate continuously, with an acceleration value depending on the aspect ratio of the pile and on the friction with the walls.

In a system with rather poorly polished walls (a surface roughness of more than $1\ \mu\text{m}$ in size), cracks occur frequently. A crack in the lower part of the pile grows, whereas a crack in the upper part is unstable and will eventually close. These experimental findings can be understood from a continuum approach based on a dynamical adaptation of Janssen's model [3,22]. Nevertheless, not all of the discontinuous phenomena, such as the reasons for the cracks, can be explained by such a continuum model. In previous works, numerical simulations were used to parallel the experiments and to analyze the falling pile for different material's parameters [22,23]. Though the simulations are dynamic, in contrast to an experiment which starts from a static situation, a reasonable phenomenological agreement was found. Furthermore, simulations were able to correlate the existence of long range cracks to strong local pressure on the walls. The increase in pressure was found to be about one order of magnitude [22]. In this work we use the numerical model of references [22–25] and investigate in detail how a crack occurs. In particular, we follow one specific crack and try to extract the generic features that could be relevant for a more involved theoretical description of the behavior of granular materials.

We briefly discuss the simulation method in Section 2 and present our results in Section 3 which consists of three main parts: firstly, we present stick-slip behavior and a local organization of the spins in Subsection 3.1. Secondly, we describe in how far the number of collisions, the kinetic energy and the pressure are connected in 3.2 and finally we present long range organization and momentum waves in Subsection 3.3. We summarize and conclude in Section 4.

2. The Simulation Method

Our simulation model is an event driven (ED) method [22,24–28] based upon the following considerations: particles undergo a parabolic flight in the gravitational field until an event occurs. An event may be the collision of two particles or the collision of one particle with a wall. Particles are hard spheres and interact instantaneously; dissipation and friction are only active on contact. Thus we calculate the momentum change using a model that is consistent with experimental measurements [28]. From the change of momentum we compute the particles' velocities after a contact from the velocities just before contact. We account for energy loss in normal direction, as for example permanent deformations, introducing the coefficient of normal restitution, ϵ . The roughness of surfaces and the connected energy dissipation, is described by the coefficient of friction, μ , and the coefficient of maximum tangential restitution β_0 . For interactions between particles and walls we use an index "w", *e.g.* μ_w . Due to the instantaneous contacts, *i.e.* the zero contact time, one may observe the so-called "inelastic collapse" in the case of strong dissipation. For a discussion of this effect see McNamara and Young [29] and

references therein. Despite this problem, we use the hard sphere ED simulations as one possible approach, since also the widely used soft sphere molecular dynamics (MD) simulations may lead to complications like the “detachment-effect” [30–32] or the so-called “brake-failure” for rapid flow along rough walls [33]. Recent simulations of the model system, described in this study, using an alternative simulation method, the so called “contact dynamics” (CD) [14], also lead to cracks [34]. The CD method has a fixed time-step, in contrast to ED where the time-step is determined by the time of the next event.

From the momentum conservation laws in linear and angular direction, from energy conservation, and from Coulomb’s law we get the change of linear momentum of particle 1 as a function of ϵ , μ , and β_0 [25]:

$$\Delta \mathbf{P} = -m_{12}(1 + \epsilon)\mathbf{v}_c^{(n)} - \frac{2}{7}m_{12}(1 + \beta)\mathbf{v}_c^{(t)}, \quad (1)$$

with the reduced mass $m_{12} = m_1 m_2 / (m_1 + m_2)$. For particle-wall interaction, we set $m_2 = \infty$ such that $m_{12} = m_1$. (n) and (t) indicate the normal and tangential components of the relative velocity of the contact points

$$\mathbf{v}_c = \mathbf{v}_1 - \mathbf{v}_2 - \left(\frac{d_1}{2}\boldsymbol{\omega}_1 + \frac{d_2}{2}\boldsymbol{\omega}_2 \right) \times \mathbf{n}, \quad (2)$$

with \mathbf{v}_i and $\boldsymbol{\omega}_i$ being the linear and angular velocities of particle i just before collision. d_i is the diameter of particle i and the unit vector in normal direction is here defined as $\mathbf{n} = (\mathbf{r}_1 - \mathbf{r}_2)/|\mathbf{r}_1 - \mathbf{r}_2|$. Paralleling ϵ , the (constant) coefficient of normal restitution we have β , the coefficient of tangential restitution

$$\beta = \min[\beta_0, \beta_1]. \quad (3)$$

β_0 is the coefficient of maximum tangential restitution, $-1 \leq \beta_0 \leq 1$, and accounts for energy conservation and for the elasticity of the material [28]. β_1 is determined using Coulomb’s law such that for solid spheres $\beta_1 = -1 - (7/2)\mu(1 + \epsilon) \cot \gamma$ with the collision angle $\pi/2 < \gamma \leq \pi$ [25]. Here, we simplified the tangential contacts in the sense that exclusively Coulomb-type interactions, i.e. $\Delta P^{(t)}$ is limited by $\mu \Delta P^{(n)}$, or sticking contacts with the maximum tangential restitution β_0 are allowed. Sticking corresponds thus to the case of low tangential velocity whilst the Coulomb case corresponds to sliding, i.e. a comparatively large tangential velocity. For a detailed discussion of the interaction model used see references [24, 25, 28].

3. Results

Since we are interested in the falling motion of a compact array of particles, we first prepare a convenient initial condition. Here, we use $N = 1562$ particles of diameter $d = 1$ mm in a box of width $L = 20.2d$, and let them relax for a time t_r under elastic and smooth conditions until the density and energy profiles do not change any longer. The choice of L is quite arbitrary, however, we wanted to start with a triangular lattice with a lattice constant of $d(1 + \Delta)$ and Δ to be small but larger than zero, i.e. $\Delta = 0.01$. We tested several height to width ratios $S = H/L$ of the system and found e.g. the same behavior as in experiments, i.e. the larger S , the stronger are the effects discussed in the following. The average velocity of the resulting initial condition is $\bar{v} = \sqrt{\langle v^2 \rangle} \approx 0.05$ m/s. The kinetic energy connected to \bar{v} is comparable to the potential energy connected to the size of one particle. Due to this rather low kinetic energy, the array of particles is arranged in triangular order, except for a few layers at the top. Some tests with different values of \bar{v} lead to similar results as long as \bar{v} is not too large.

The larger \bar{v} , the more particles belong to the fluidized part of the system at the top and in the fluidized part of the system we can not observe cracks. For lower values of \bar{v} we observed an increasing number of events per unit time and thus increasing computational costs for the simulation. At $t = 0$ we remove the bottom, switch on dissipation and friction and let the array fall.

Performing simulations with different initial conditions and different sets of material's parameters, we observe differences in position and shape of the cracks. However, the intensity or the probability of the cracks seems to depend on the material's parameters rather than on the initial conditions. The behavior of the system depends on friction and on dissipation as well: for weak friction we observe only random cracks, which would occur even in a dense hard sphere gas without any friction, simply due to random fluctuations and the internal pressure. With increasing friction, cracks may even span the whole system and sometimes be correlated to slip planes. Furthermore, we observe cracks to occur more frequent for lower dissipation.

In Figure 1a we present typical snapshots of an experiment and of a simulation at time $t = 0.04$ s. We observe long range cracks from both, experiments and simulations as well. For the experiment we use a container of width $L/d = 24$ with 103 layers of oxidized aluminum particles. The vertical 2D cell is made up of two glass windows for visualisation and of two lateral walls made of plexiglass. The gap between the glass windows is a little larger than the bead diameter, what leads to a small friction between particles and front/back walls, while the friction with the side walls may be large. Different heights and wall-materials were used and the results could be scaled with a characteristic length $\xi = L/(2K\mu_w)$, with the dimensionless parameter K which characterizes the conversion of vertical to tangential stresses and the coefficient of friction μ_w . The scaling in the regime before cracks occur leads to the value $K\mu_w \approx 0.12$. For a more detailed description of the experimental setup and data see reference [22]. In the simulation of Figure 1a we have $N = 1562$ and the parameters $L/d = 20.2$, $\epsilon = 0.96$, $\epsilon_w = 0.92$, $\mu = 0.5$, $\mu_w = 1.0$, and $\beta_0 = \beta_{0w} = 0.2$. We varied the coefficients of friction in the intervals $0 \leq \mu \leq 1$ and $0 \leq \mu_w \leq 10$. Furthermore, we varied the coefficients of restitution in the range $0.80 \leq \epsilon$ or $\epsilon_p \leq 0.98$. However, the occurrence of cracks is quite independent of the parameters used, as long as the coefficients of friction, μ and μ_w are sufficiently large. Furthermore, cracks occur faster for stronger dissipation since a highly dissipative block dissipates the initial energy faster.

For the above parameters, we find — like in experiments — a large number of cracks, overlapping and interfering. In the upper part of both, experiment and simulation, we sometimes observe cracks only on one side. In contrast to Figure 1a we present in Figure 1b a specific simulation with only one strong crack, on which we focus in more detail. This crack separates the system into a large upper and a small lower part and is best visible in Figure 1b at $t = 0.068$ s. Here we use a reduced wall friction, *i.e.* $\mu_w = \mu = 0.5$, and stronger dissipation, *i.e.* $\epsilon_w = \epsilon = 0.9$, while all other parameters, including the initial configuration, are the same as for (a).

In order to distinguish consistently, we will refer to the simulation with large μ_w as simulation (a), and to the simulation with small μ_w as simulation (b) in the following.

The important feature of the crack in Figure 1b is that it seems to be connected to one single particle. We indicate the vertical position of particle #371 with a small bar in Figure 1b. The crack of simulation (b) is connected to an increase of the number of collisions per particle, indicated by the greyscale on Figure 1b. Black or white correspond to zero or more than twenty collisions during the last millisecond respectively. Note that the increase in the number of collisions is here equivalent to an increase in pressure. Already at time $t = 0.048$ s, particle #371 performs more collisions than the average particle. The pressure around particle #371 increases and at $t = 0.056$ s a region in which the particles perform a large number of collisions

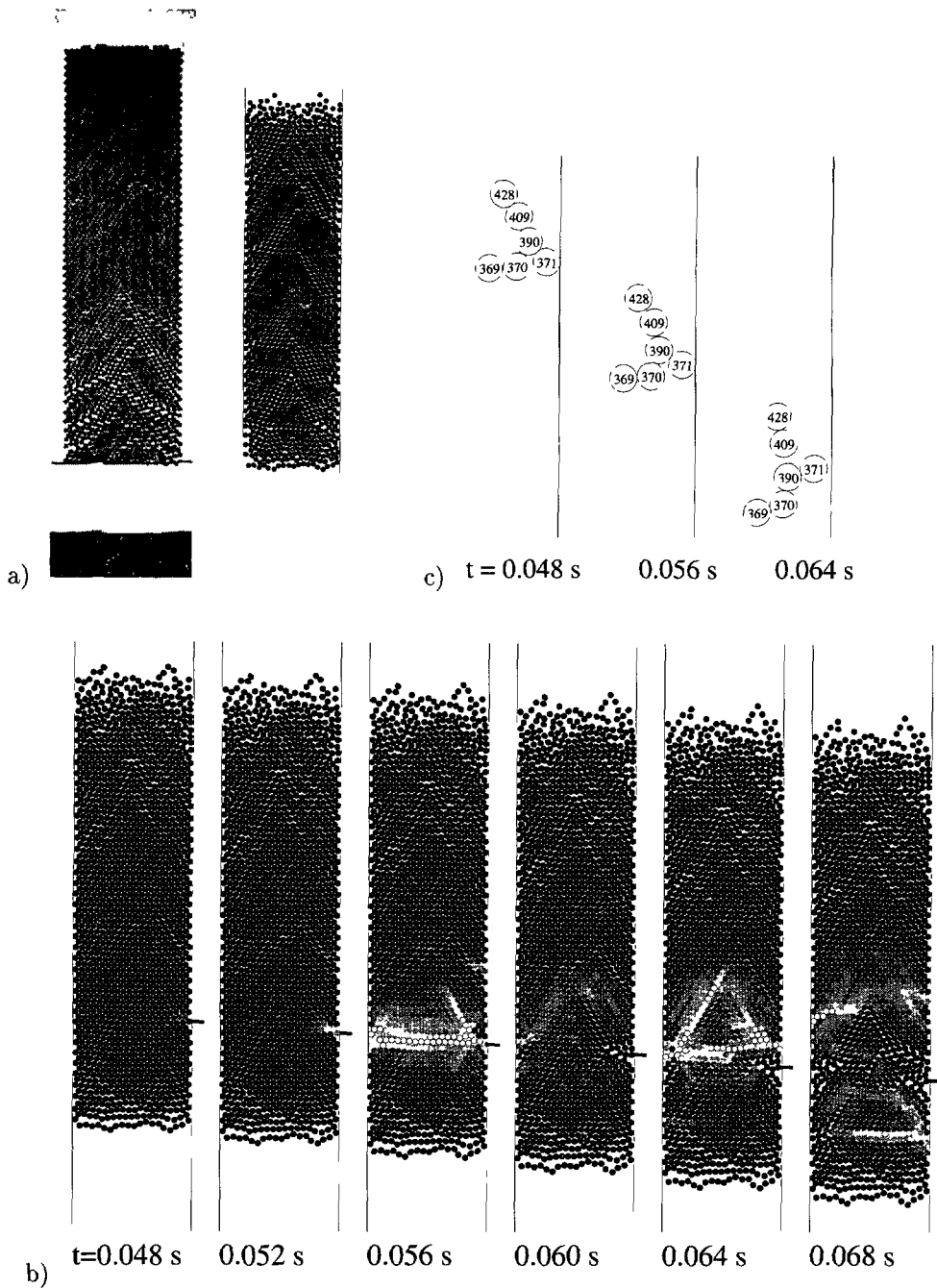


Fig. 1. — a) Snapshots of a typical experiment (left) and a simulation (right) with $n = 1562$ particles, at times $t = 0.06$ s, in a pipe of width $L/d = 20.2$. We used here $\epsilon_w = 0.92$, $\mu = 0.5$, $\mu_w = 1.0$, and $\beta_0 = \beta_{0w} = 0.2$. b) Snapshots from a simulation with almost the same parameters as in (a), but here $\epsilon = 0.90$, $\epsilon_w = 0.90$, and $\mu_w = 0.5$. The greyscale indicates the number of collisions per particle per millisecond. Black and white correspond to no collision or more than ten collisions respectively. c) Here only the selected particles #369, #370, #371, #390, #409, and #428 from (b) are plotted to illustrate their motion. The vertical line indicates the right wall.

spans the whole width of the container. We call such an array of particles under high pressure “dynamic arch”. At $t = 0.060$ s the pressure decreases and a large crack opens below particle #371. At later times, we observe new pressure fluctuations in the array. In conclusion, a crack seems to begin at one point, *i.e.* one particle, where the pressure increases accidentally.

Before we look in more detail at the behavior of particle #371, we present for convenience, a picture of some selected particles around #371 from (b), in Figure 1c.

3.1. EVIDENCE FOR STICK-SLIP BEHAVIOR. — From Figure 1b we evidenced that a crack may originate from one particle only. Now we are interested in the velocity of one specific particle during its fall. Following the order of simulations (a) and (b) we firstly present the case of large wall friction (a) and secondly the case of smaller wall friction (b) in the following. Remember that particle #371 is the origin of one single crack in simulation (b), while its behavior is similar to the behavior of many others, close to the boundary, in simulation (a).

Due to gravity, the particle is accelerated downwards and after a collision with the right wall it will presumably rotate counterclockwise. Therefore, we compare the linear velocity, V_z , with the rotational velocity of the surface, ωr . In Figure 2 we plot both, the linear vertical and the angular velocity of particle #371 as a function of time. The horizontal line indicates zero velocity and the diagonal line indicates the free fall velocity, $-gt$. The full curve gives the (negative) linear velocity in vertical direction, V_z , while the rotational velocity of the surface, ωr , is given by the dashed curve. Negative ωr values correspond to counterclockwise rotation and for $V_z = \omega r$ we have the contact point of the particle at rest relative to the wall. The particle adapts rotational and linear velocity, or in other words, the contact point sticks. This event occurs when the two curves merge. In Figure 2a we observe a small angular velocity up to $t \approx 0.02$ s when particle #371 first sticks. Note that in this simulation (a) #371 can not be identified as the initiator of one of the numerous cracks; however, it sticks and slips several times. An increase in angular velocity goes ahead with a decrease of linear velocity due to momentum conservation. At larger times we observe the angular velocity decreasing, *i.e.* the particle slips, and short time after, sticks again.

Now we focus on simulation (b) and the behavior of the particle, from which the crack started. In Figure 2b we observe a small angular velocity up to $t \approx 0.050$ s. At $t = 0.055$ s the velocities are adapted for some 0.005 s before the particle slips again. Since the pressure fluctuations are visible in Figure 1b already at $t = 0.048$ s, we conclude that pressure fluctuations in the bulk lead to a sticking of a particle surface on the wall. This particle is slowed down and thus will perform more collisions with those particles coming from above, what leads to an increase of pressure. An increase of pressure allows, in general, a strong Coulomb friction and thus a sticking of the contact point. When pressure decreases, the particle surface does not longer stick on the wall.

Since the sticking might also occur between particles, we examine the angular velocity of the particles in the neighborhood of the sticking particle, *i.e.* the particles to the upper left of particle #371. In Figure 3 we plot the angular velocities of particles #371, #390, #409, and #428 for the simulations (a) and (b). We observe from both figures as a response to friction, an auto-organization of the spins as also observed in 1D experiments and simulations of rotating frictional cylinders [12, 13]. Spin stands here for the direction of angular velocity of a particle. We see that the direct neighbor of #371 to the left and upwards, *i.e.* #390, rotates in the opposite direction of #371. Thus a counterclockwise rotation of particle #371 leads to a clockwise rotation of #390. This is consistent with the idea of friction reducing the relative surface velocity. The next particle to the upper left, *i.e.* #409, is again rotating counterclockwise, following the same idea of frictional coupling. In Figure 3a we observe only a weak coupling between #409 and #428, whereas in Figure 3b particle #428 is also rotating

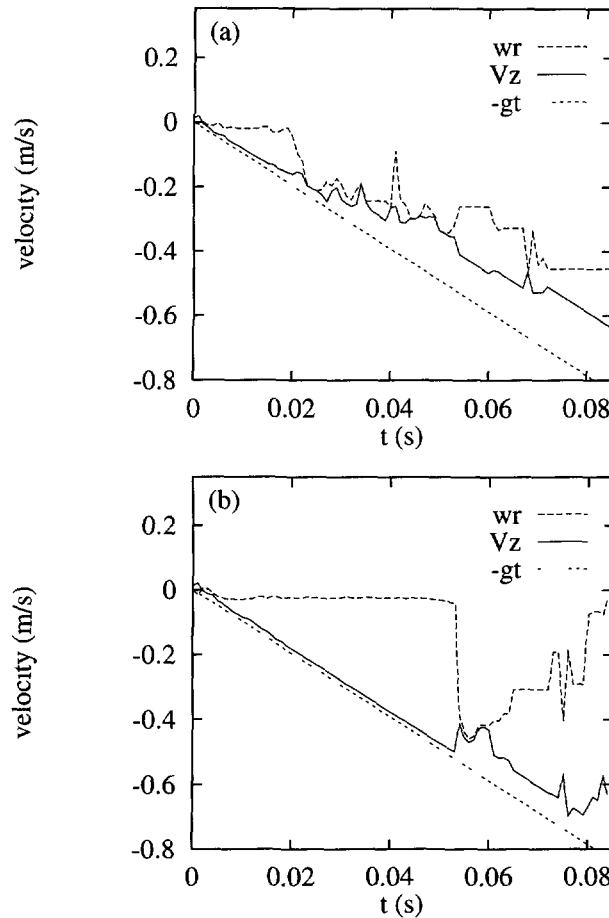


Fig. 2. — Plot of the angular velocity, ω_r , and of the linear, vertical velocity, V_z , of particle #371 versus time. The simulations are the same as in Figure 1a and 1b. The line $-gt$ corresponds to a freely falling particle.

clockwise, even when the absolute value of the angular velocity is smaller. Thus we have not only a stick-slip behavior of particles close to the side walls, but also a coupling of the spins of neighboring particles. If the coupling is strong enough, we observe an alternating, but decreasing angular velocity along a line. We will return to this observation in Subsection 3.3.

3.2. NUMBER OF COLLISIONS, KINETIC ENERGY AND PRESSURE. — Since the occurrence of a crack is, in general, connected to a large number of collisions, we plot in Figure 4 the number of collisions per particle per millisecond, N_c , for simulations (a) and (b). In Figure 4a we observe an increase in the number of collisions, which is related to the first sticking event of particle #371. However, particles deep in the array possibly perform much more collisions, see #428 in Figure 4a. Obviously, an increase in N_c for one particle is connected to an increase in N_c for the neighbors. In Figure 4b we find values of N_c comparable for direct neighbors, *i.e.* #371 and #390. At $t = 0.056$ s we observe a drastic increase in N_c which also involves the particles deeper in the array, *i.e.* #409 and #428.

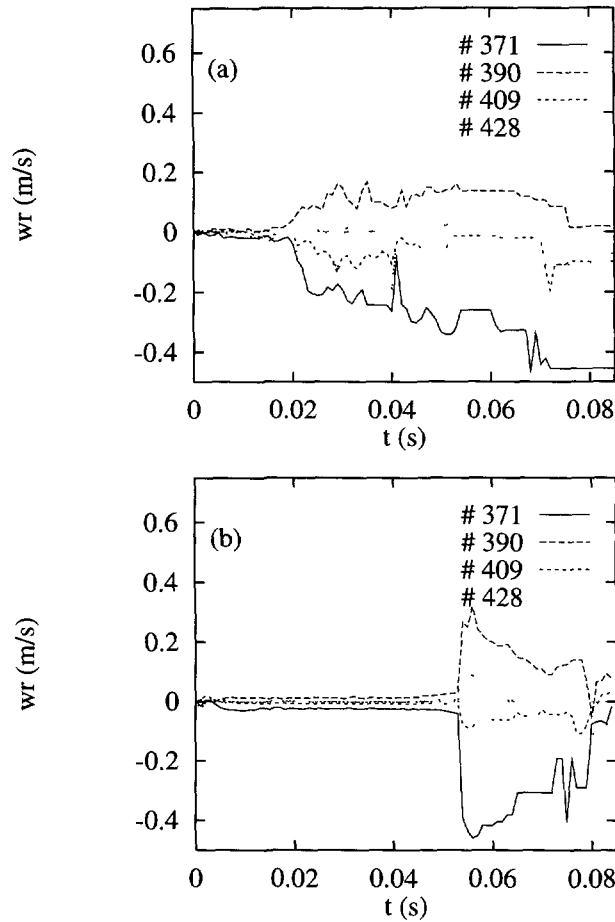


Fig. 3. — Plot of the angular velocities of the particles #371, #390, #409, and #428 for the same simulations as in Figure 1a and 1b. These particles were initially arranged on a line, tilted clockwise by 60 degrees from the horizontal, see Figure 1c.

In order to illustrate the reduced falling velocity, connected to a large number of collisions we plot in Figure 5 the averaged kinetic energy K for particles between heights z and $z + dz$ (we use here $dz = 0.002$ m). We plot $K = (1/N)\sum_{i=1}^N v_i^2$ (disregarding the mass of the particles), as a function of the height, z . Note that v_i is the velocity of one particle relative to the walls, and not relative to the center of mass of the falling sandpile. We observe different behavior for the simulations (a) and (b): a rather homogeneous deceleration of the pile in (a) and one “dynamic arch” connected to a strong deceleration in (b). For strong friction at the walls (a), all particles in the system are slowed down due to frequent collisions of the particles with the side walls and inside the bulk. For the times $t = 0.05$, 0.06 , and 0.08 s we observe, from the bottom indicated by the left vertical line in Figure 5, a decreasing K with increasing height z up to $z \approx 0.02$ m, where the slope of K almost vanishes. In Figure 5b the particles are falling faster at the beginning until the first dynamic arch occurs at $t \approx 0.056$ s, see Figure 1b. The high pressure exerted on the walls, together with the tangential friction at the walls, leads to a local deceleration, *i.e.* the dip in the K profile for $t = 0.06$ s. This dip identifies a dynamic

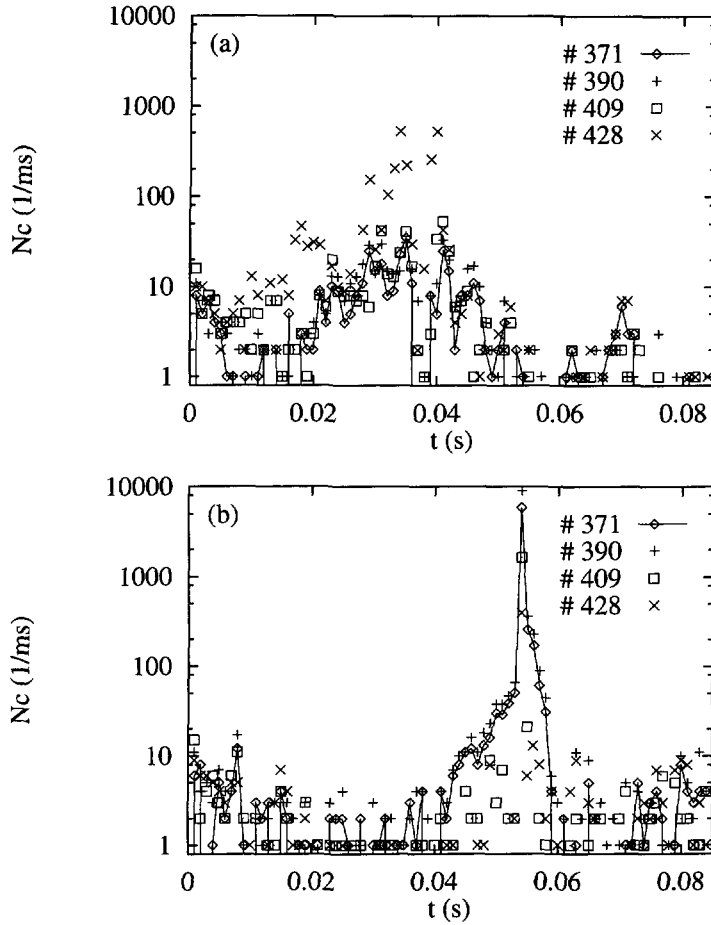


Fig. 4. — Log-lin plot of the number of collisions, N_c , per millisecond (ms) as a function of simulation time, t . Plotted is N_c for the four particles noted in the figure. The data are from the same simulations as already presented in Figure 1a and 1b.

arch of slow material which temporarily blocks the flow. Later in time, the particles from above arrive at the slower dynamic arch, which again leads to great pressure, a large number of collisions and thus to a further reduction of K (see the K profile for $t = 0.08$ s).

In order to understand how the pressure in the bulk is connected to N_c and K we plot in Figure 6 the particle-particle pressure, pp , in arbitrary units as a function of height for the simulations (a) and (b). pp is here defined as the sum over the absolute normal part of momentum change

$$pp(z, t) = \Sigma |\Delta \mathbf{P}^{(n)}|, \tag{4}$$

for each particle in a layer $[z, z + dz]$ in a time interval $[t, t - dt]$. For this plot we use $dz = \sqrt{3}d$ (what corresponds to a height of two particle layers) and the integration time is here $dt = 0.005$ s. For strong wall friction and low dissipation (a), we observe already at $t = 0.02$ s a quite strong pressure with a maximum close to the bottom of the pile. At $t = 0.05$ s the maximum in pressure moved upwards, not only within the falling pile but also in coordinate z . Furthermore, the maximum is about one order of magnitude larger than before. Later, the

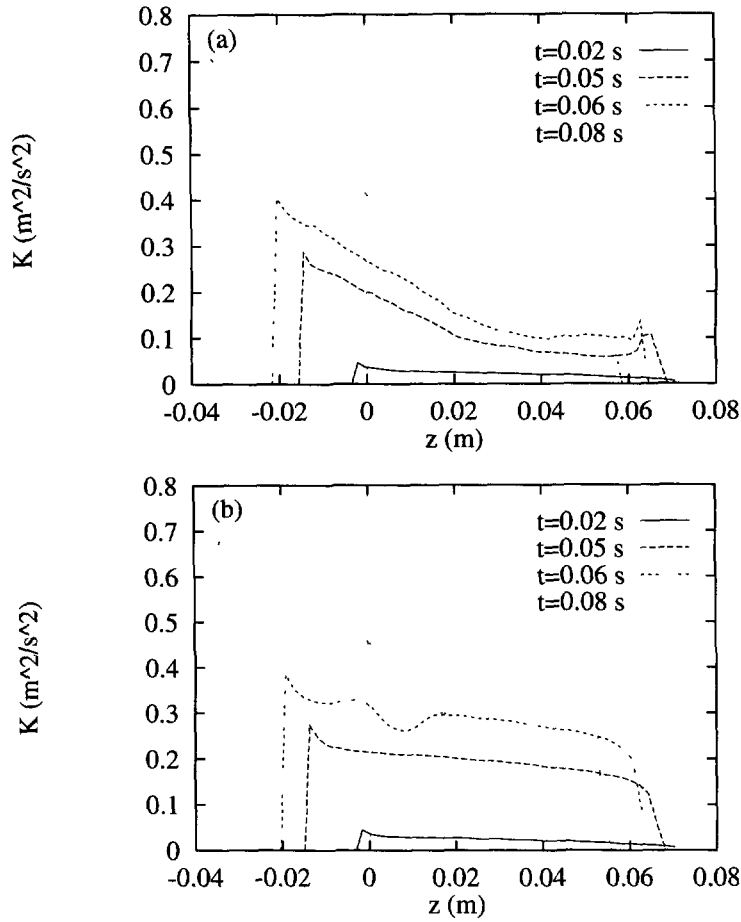


Fig. 5. — Plot of the kinetic energy K as a function of height z for different times for the same simulations as already presented in Figure 1a and 1b.

pressure peak moved further upwards and at $t = 0.06 \text{ s}$ begins to decrease until at larger times the array is dilute and pressure almost vanished. For weak wall friction (b) we find only a weak pressure at time $t = 0.02 \text{ s}$ until at time $t = 0.06 \text{ s}$ a sudden increase of pressure, connected to the increase in N_c and the decrease in K , appears. The occurrence of two pressure peaks of different amplitude (small pressure at the bottom and large pressure at the top) is consistent with the predictions of Duran *et al.* [22], which state that a small lower pile will be decelerated less than a large upper pile. Thus the crack continues opening.

3.3. LONG RANGE ROTATIONAL ORDER AND MOMENTUM WAVES. — We have learned from Figures 2 and 3 that, connected to a large number of collisions, the direction of the angular velocity, *i.e.* the spin of the particles, may be locally arranged in an alternating order along lines of large pressure. In order to proof that this is not only a random event we plot in Figure 7a one snapshot from simulation (a) and indicate clockwise and counterclockwise rotation with black and white circles respectively. We observe, at least in some parts of the system, that spins of the same direction are arranged along lines. The spins of two neighboring lines have different

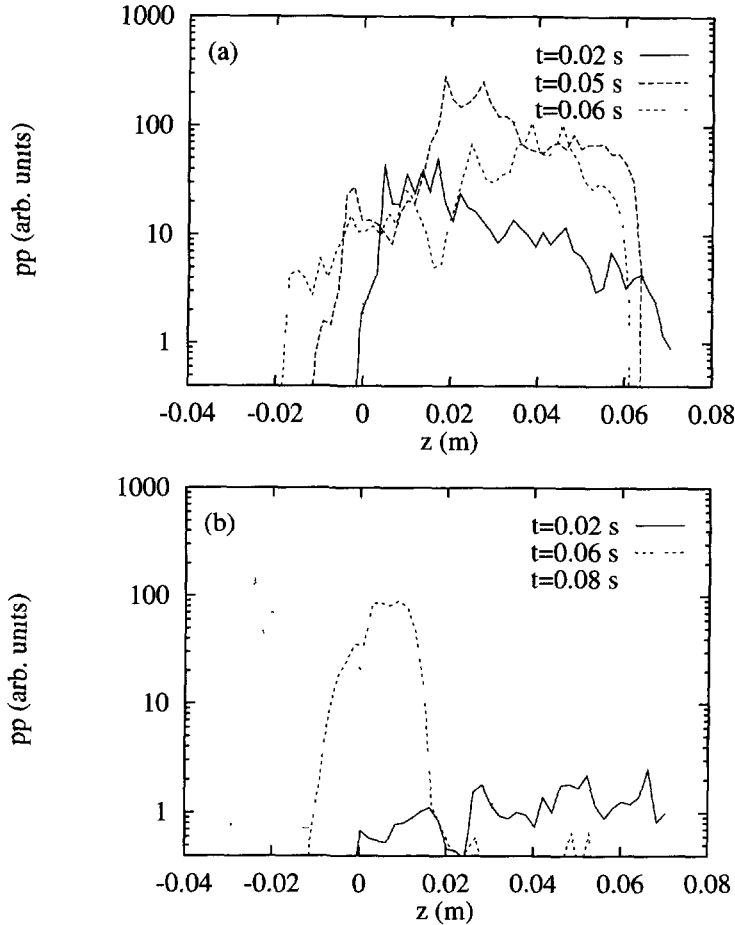


Fig. 6. — Log-lin plot of the pressure, pp , as a function of height z for different times for the same simulations as already presented in Figure 1a and 1b.

directions. The elongation of the ordered regions may be comparable to the horizontal size of the system. Note, that lines of equal spin are perpendicular to a line of strong pressure, such that the order in Figure 7a indicates an arch like structure. For recent analytic predictions of the shape of arches see [35].

In Figure 7b we plot snapshots from simulation (b) and plot the change of velocity, *i.e.* $\Delta v_x = v_x(t + \delta t) - v_x(t)$ and $\Delta v_z = v_z(t + \delta t) - v_z(t) + g \delta t$ with $\delta t = 10^{-3}$ s. Comparing Figures 1b and 7b we identify the large number of collisions, starting from particle #371, with a momentum wave propagating from #371 towards the left wall and also diagonally upwards. When the momentum wave arrives at the left wall it is reflected and moves mainly upwards. We relate this to the fact that the material below the dynamic arch is falling faster than the dynamic arch, such that not much momentum change takes place downwards. After several milliseconds the momentum wave is not longer limited to some particles only, but has spread and builds now an active region with great pressure, *i.e.* the dynamic arch.

Examining the rotational order in simulation (b), we observe that the spin order is a consequence of the momentum wave. In our model, strong coupling is related to a large number

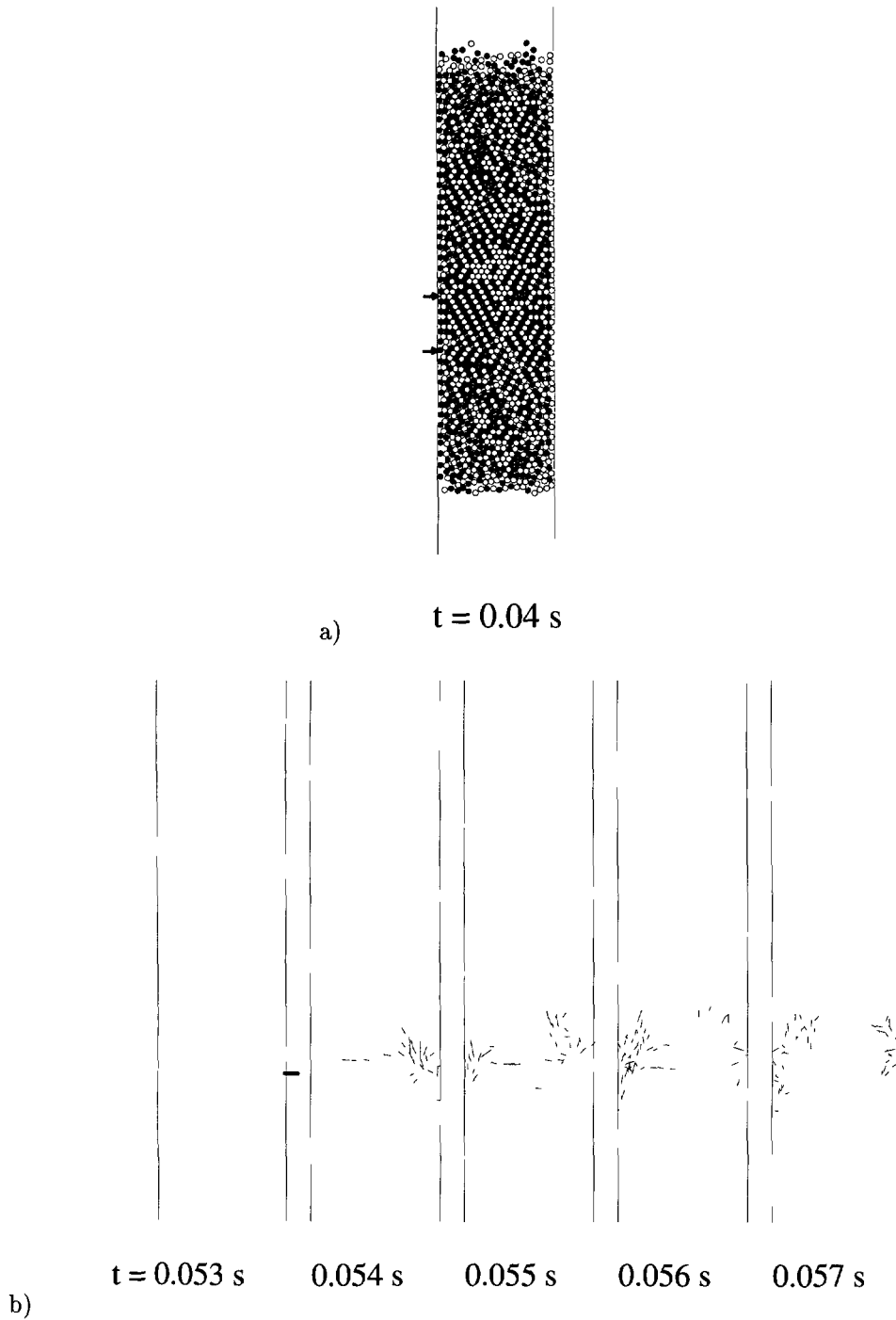


Fig. 7. — a) Snapshots of the simulation from Figure 1a at time $t = 0.04 \text{ s}$. The color indicates here the direction of the angular velocity, i.e. black and white correspond to clockwise and counterclockwise rotation respectively. b) Snapshots from the simulation from Figure 1b at different times. The lines indicate for each particle the change in velocity due to collisions within the last millisecond.

of collisions and thus to a large pressure. This is due to the fact, that informations about the state of the particles are exchanged only on contact. Therefore, lines of equal spin are mostly perpendicular to the lines of great pressure, a finding that is also discussed in reference [14].

4. Summary and Conclusion

We presented simulations of a 2D granular model material, falling inside a vertical container with parallel walls. We observe fractures in the material which were described as a so-called “discontinuous decompaction” which is the result of many cracks breaking the granular assembly into pieces from the bottom to the top. The case of high friction and quite low dissipation (a) is a system which shows the same behavior as also found in various experiments. Many cracks occur and interfere. When we investigate an exemplary situation with rather low friction and high dissipation (b) we observe one isolated crack. We followed in detail the events which lead to this crack. Due to fluctuations of pressure (equivalent to fluctuations in the number of collisions, N_c), some particles may transfer a part of their linear momentum into rotational momentum. This happens when the surface of a particle with small angular velocity sticks on the wall. Sticking means here that the velocities of particle surface and wall surface are adapted.

The momentum wave, starting from such a particle, leads to a region of large pressure, which spans the width of the system, *i.e.* a dynamic arch. Due to the strong pressure, the dynamic arch is slowed down by friction with the walls. The material coming from above hits the dynamic arch such that a density and pressure wave, propagates upwards inside the system.

Under conditions with quite strong wall friction and rather weak dissipation, the fluctuations in the system and also the coupling with the walls are greater, such that many particles are sticking on the walls. This leads to several pressure waves, interfering with each other such that the system is slowed down more homogeneously.

With the dynamic simulations used, we were able to reproduce the experimentally observed discontinuous decompaction [22] and to propose an explanation, how the cracks occur. The open question remains, if the situation discussed here is relevant for all types of experiments in restricted geometries. The features described here, *i.e.* rotational order, stick-slip behavior, and momentum waves are not yet observed in experiments. Besides, the phenomenon of stress fluctuations has been shown to be important for both, the behavior of static [16] and of quasistatic granular systems [15]. Furthermore, the behavior of cracks in polydisperse or three dimensional systems is still an open problem.

Acknowledgments

We thank S. Roux for interesting discussions and gratefully acknowledge the support of the European Community (Human Capital and Mobility) and of the PROCOPE/APAPE scientific collaboration program. The group is part of the French Groupement de Recherche sur la Matière Hétérogène et Complexe of the CNRS and of a CEE network HCM.

References

- [1] Jaeger H.M. and Nagel S., *Science* **255** (1992) 1523.
- [2] Jaeger H.M., Knight J.B., Liu C.h. and Nagel S.R., *MRS Bulletin* **5** (1994) 25.

- [3] Brown R.L. and Richards J.C., Principles of Powder Mechanics (Pergamon Press, Oxford, 1970).
- [4] Baxter G.W., Behringer R.P., Fagert T. and Jonhson G.A., *Phys. Rev. Lett.* **62** (1989) 2825.
- [5] Baxter G.W., Leone R. and Behringer R.P., *Europhys. Lett.* **21** (1993) 569.
- [6] Pöschel T., *J. Phys. I France* **4** (1994) 499.
- [7] Peng G. and Herrmann H.J., *Phys. Rev. E* **49** (1994) 1796.
- [8] Lee J. and Leibig M., *J. Phys. I France* **4** (1994) 507.
- [9] Raafat T., Hulin J.P. and Herrmann H.J., to be published in *Phys. Rev. E*.
- [10] Jenkins J. and Savage S., *J. Fluid Mech.* **130** (1983) 186.
- [11] Lun C., Savage S., Jeffrey D. and Chepurniy N., *J. Fluid Mech.* **140** (1984) 223.
- [12] Radjai F. and Roux S., *Phys. Rev. E* **51** (1995) 6177.
- [13] Radjai F., Evesque P., Bideau D. and Roux S., *Phys. Rev. E* **52** (1995) 5555.
- [14] Radjai F., Brendel L. and Roux S. (unpublished).
- [15] Pouliquen O. and Gutfraind R., *Phys. Rev. E* **53** (1996) 552.
- [16] Liu C.h. *et al.*, *Science* **269** (1995) 513.
- [17] Duran J., Mazozi T., Clément E. and Rajchenbach J., *Phys. Rev. E* **50** (1994) 3092.
- [18] Knight J.B., Jaeger H.M. and Nagel S.R., *Phys. Rev. Lett.* **70** (1993) 3728.
- [19] Clément E., Duran J. and Rajchenbach J., *Phys. Rev. Lett.* **69** (1992) 1189.
- [20] Warr S., Jacques G.T.H. and Huntley J.M., *Powder Technology* **81** (1994) 41.
- [21] Cantelaube F., Duparcmeur Y.L., Bideau D. and Ristow G.H., *J. Phys. I France* **5** (1995) 581.
- [22] Duran J. *et al.*, *Phys. Rev. E* **53** (1996) 1923.
- [23] Luding S. *et al.*, in Traffic and Granular Flow, D.E. Wolf Ed. (Forschungszentrum Jülich, Jülich, Germany, 1995).
- [24] Walton O.R., in Particulate Two Phase Flow, M.C. Roco Ed. (Butterworth-Heinemann, Boston, 1992).
- [25] Luding S., *Phys. Rev. E* **52** (1995) 4442.
- [26] Lubachevsky B.D., *J. Comp. Phys.* **94** (1991) 255.
- [27] Luding S., Herrmann H.J. and Blumen A., *Phys. Rev. E* **50** (1994) 3100.
- [28] Foerster S.F., Louge M.Y., Chang H. and K. Allia, *Phys. Fluids* **6** (1994) 1108.
- [29] McNamara S. and Young W.R., to be published in *Phys. Rev. E*.
- [30] Luding S. *et al.*, *Phys. Rev. E* **50** (1994) R1762.
- [31] Luding S. *et al.*, *Phys. Rev. E* **50** (1994) 4113.
- [32] Luding S. *et al.*, in Fractal Aspects of Materials, F. Family, P. Meakin, B. Sapoval and R. Wool Eds. (Materials Research Society, Symposium Proceedings, Pittsburgh, Pennsylvania, 1995) Vol. 367.
- [33] Schaefer J. and Wolf D.E., *Phys. Rev. E* **51** (1995) 6154.
- [34] Moreau J.J., private communication (unpublished).
- [35] Mounfield C.C. and Edwards S.F., *Physica A* to appear.